INL/JOU-24-82408-Revision-1

# Comprehensive Toughness Dataset of Nuclear Reactor Structural Materials using Charpy V-Notch Impact Testing

April 2025

Isshu Lee, Yugandhar Kasala, Fei Xu, Yalei Tang, Joshua Eddy Rittenhouse, Rongjie Song, Aleksandar Vakanski, John Wesley Merickel

Changing the World's Energy Future

Idaho National Laboratory

*INL is a U.S. Department of Energy National Laboratory operated by Battelle Energy Alliance, LLC*

INL/JOU-24-82408-Revision-1

# Comprehensive Toughness Dataset of Nuclear Reactor Structural Materials using Charpy V-Notch Impact Testing

**Isshu Lee, Yugandhar Kasala, Fei Xu, Yalei Tang, Joshua Eddy Rittenhouse, Rongjie Song, Aleksandar Vakanski, John Wesley Merickel**

**April 2025**

**Idaho National Laboratory**
**Idaho Falls, Idaho 83415**

**http://www.inl.gov**

**Prepared for the**
**U.S. Department of Energy**
**Under DOE Idaho Operations Office**
**Contract DE-AC07-05ID14517**

scientific data

Check for updates

OPEN

DATA DESCRIPTOR

# Comprehensive Toughness Dataset of Nuclear Reactor Structural Materials using Charpy V-Notch Impact Testing

Isshu Lee[1,3], John W. Merickel[1,3], Yugandhar Kasala Sreenivasulu[2,3], Fei Xu[1], Yalei Tang[1], Joshua E. Rittenhouse[1], Aleksandar Vakanski[2]✉ & Rongjie Song[1]✉

**Reactor pressure vessel (RPV) steels are critical for maintaining the structural integrity and safety of nuclear reactors, designed to endure extreme conditions over prolonged operational lifetimes. Evaluating the mechanical properties of RPV steels frequently involves tests with sub-sized specimens, due to size constraints associated with irradiated materials. However, the reduced specimen dimensions introduce a size effect that alters material behavior and requires correlating the test results to full-sized specimens. Although numerous correlation methods have been previously proposed, they are typically applicable to specific test conditions. To address these challenges, this study introduces a public dataset of 4,961 Charpy impact test records for RPV steels. The dataset was compiled through a comprehensive literature review and incorporates data from 109 peer-reviewed publications. It provides detailed information on material composition, manufacturing treatments, specimen dimensions, testing conditions, and test results. The primary objective of the dataset is to advance the understanding of specimen size effect in Charpy impact testing, and support studies for validating existing methods and developing data-driven approaches for test results correlation.**

## Background & Summary

Nuclear power remains one of the most significant contributors to global energy production in the 21st century. The continued safe operation and advancement of nuclear power plants rely significantly on the research and development of reactor pressure vessel (RPV) materials[1,2]. Current research efforts in the nuclear sector are increasingly directed toward designing advanced high-efficiency reactors with extended operational lifespans[3–5]. The next-generation reactors are being engineered to operate at significantly higher temperatures and radiation flux levels than their predecessors, which necessitates the development of novel materials with superior performance under extreme environments.

One of the main challenges in materials research for advancing the nuclear sector is the constrained volume and geometrical limitations of test reactors, which preclude the use of standard-sized specimens for conducting mechanical tests[5,6]. Furthermore, the expanding complexity of material development and testing has led to significant increases in the associated costs and time requirements for producing testing materials. To address these challenges, reducing the size of test specimens has emerged as a practical mitigation strategy, enabling to perform greater number of tests with limited material resources, thereby accelerating the pace of research and development[7–17].

Sub-sized specimens have been extensively employed to characterize material performance over the last four decades. Despite the advantages, testing with sub-sized specimens presents unique challenges, including the need for test instrumentation with higher resolution and precision to ensure accurate measurements, and increased variability in mechanical properties caused by microstructural heterogeneity at smaller scales[18–20]. One of the most significant challenges associated with sub-sized specimen testing is the phenomenon of specimen size effect, referring to altered material behavior due to scaling or geometrical changes in the test samples[8,21].

[1]Idaho National Laboratory, Idaho Falls, ID, USA. [2]Department of Computer Science, University of Idaho, Moscow, ID, USA. [3]These authors contributed equally: Isshu Lee, John W. Merickel, Yugandhar Kasala Sreenivasulu. ✉e-mail: vakanski@uidaho.edu; rongjie.song@inl.gov

| | | C | Si | Mn | P | S | Ni | Cr | Mo | V | Cu | Fe |
|---|---|---|---|---|---|---|---|---|---|---|---|---|
| SA533B | min | 0 | 0.15 | 0.80 | 0 | 0 | 0.37 | — | 0.35 | — | — | Balance |
| | max | 0.25 | 0.60 | 1.80 | 0.035 | 0.035 | 0.85 | — | 0.65 | — | — | Balance |
| SA508 | min | 0.15 | 0.15 | 0.66 | 0.006 | 0 | 0.37 | 0.31 | 0.37 | — | 0.03 | Balance |
| | max | 0.21 | 0.30 | 1.59 | 0.012 | — | 0.85 | 0.45 | 0.68 | 0.01 | 0.10 | Balance |
| 20MnMoNi55 | min | 0.17 | 0 | 1.00 | 0 | 0 | 0.40 | — | 0.45 | — | — | Balance |
| | max | 0.23 | 0.35 | 1.50 | 0.020 | 0.020 | 0.80 | 0.30 | 0.60 | — | 0.18 | Balance |
| A302B | min | 0 | 0.13 | 1.07 | 0 | 0 | — | | 0.41 | — | — | Balance |
| | max | 0.25 | 0.45 | 1.62 | 0.035 | 0.035 | — | — | 0.64 | — | — | Balance |
| SS316 | min | 0 | 0 | 0 | 0 | 0 | 10.0 | 16.0 | 2.00 | — | — | Balance |
| | max | 0.08 | 0.75 | 2.00 | 0.045 | 0.030 | 14.0 | 18.0 | 3.00 | — | — | Balance |

**Table 1.** Chemical compositions of the studied alloys, weight %.

Failure to account for the size effect can result in inaccurate reporting of material properties, posing potential premature material fracture and safety risks.

For structural integrity assessment, the Charpy V-Notch (CVN) impact test is one of the simplest and most cost-effective methods to determine key material properties, such as upper shelf energy (USE), and ductile-to-brittle transition temperature (DBTT). Sub-sized Charpy specimens have been increasingly adopted to address the limited availability of irradiated material samples and extend current surveillance programs (e.g., by manufacturing specimens with reduced size from broken halves of previously tested full-sized specimens[22]). On the other hand, testing with sub-sized Charpy specimens causes a shift in characteristic parameters like USE and DBTT compared to full-sized specimens. Consequently, multiple analytical methods have been developed to correlate test parameters between sub-sized and full-sized Charpy specimens. These analytical methods were employed by application standards such as ASTM A370[23], BS7910[24], and API57[25] to provide guidelines for converting experimental data from sub-sized Charpy specimens to correspond to full-size specimen results. However, current conversion methods typically rely on applying simple scaling factors or power-law relations to the experimentally obtained results, and struggle to accurately correlate the effect of reduced specimen dimensions across the entire ductile-to-brittle transition range. For example, sub-sized specimens tend to produce higher impact energies in the lower shelf region and proportionally lower energies in the upper shelf region[20]. Additionally, conversion methods that employ empirical relations require determining correlation parameters, which are dependent on the used material and test conditions; hence, the correlation parameters need to be determined based on empirical results for each new material and test condition[26]. The development of advanced methods for correlating Charpy impact test results between sub-sized and full-sized specimens that reliably model the complex interaction between ductile and brittle fracture mechanisms remains an open research question.

Recent advances in machine learning (ML) have the potential to address the complexities associated with specimen size effect in material testing. Specifically, ML-based approaches excel in pattern recognition and can account for the non-linear relationships among high-dimensional features in sub-sized specimen testing[27–29]. For instance, ML methods can integrate categorical features into model training (such as specimen orientation, manufacturing treatment, and microstructural characteristics), which are difficult to incorporate into conventional analytical correlation models, but can otherwise significantly impact test outcomes[30–35]. Furthermore, explainable ML techniques allow researchers to interpret the contributions of individual variables (such as composition and testing temperature) to the test results and can provide valuable insights for associating experimental observations with the specimen size effect.

This paper aims to lay the groundwork for future studies that explore the size effect on Charpy specimens. Toward this goal, we created a public dataset of Charpy impact test properties for RPV steels and nuclear structural materials, including SA533B, SA508, 20MnMoNi55, A302B, and SS316 alloys. The chemical compositions of these alloys are shown in Table 1. The dataset consists of 4,961 Charpy test records and provides detailed information on material composition, manufacturing treatments, irradiation conditions, specimen dimensions, testing conditions, and Charpy impact test results. The dataset was compiled through a comprehensive literature review and incorporates data from 109 peer-reviewed publications. The search inclusion criteria targeted peer-reviewed studies on Charpy-impact testing of sub-sized and full-sized specimens, providing quantitative data on material properties relative to specimen size. Material science experts performed technical validation to verify the accuracy and consistency of collected data. The dataset of Charpy impact tests can be leveraged to validate existing analytical methods or develop ML predictive models for establishing correlations between sub-sized and full-sized specimen properties. Such models can contribute to extending the safe operational lifespans of nuclear reactors and ensuring the reliability of structural materials under extreme conditions.

## Methods

**Charpy V-notch Impact Test.** The Charpy impact test is a standardized method for evaluating the impact toughness of materials under dynamic loading conditions. Developed by Georges Augustin Albert Charpy in the early 1900s[36], the test enables high strain rate mechanical assessments across a range of temperatures, offering important insights into material toughness and fracture behavior.

In the Charpy test, a notched specimen is placed horizontally on two supports, and a pendulum hammer set at a fixed height is released to strike the specimen opposite the notch and fracture it (see Fig. 1a). The energy

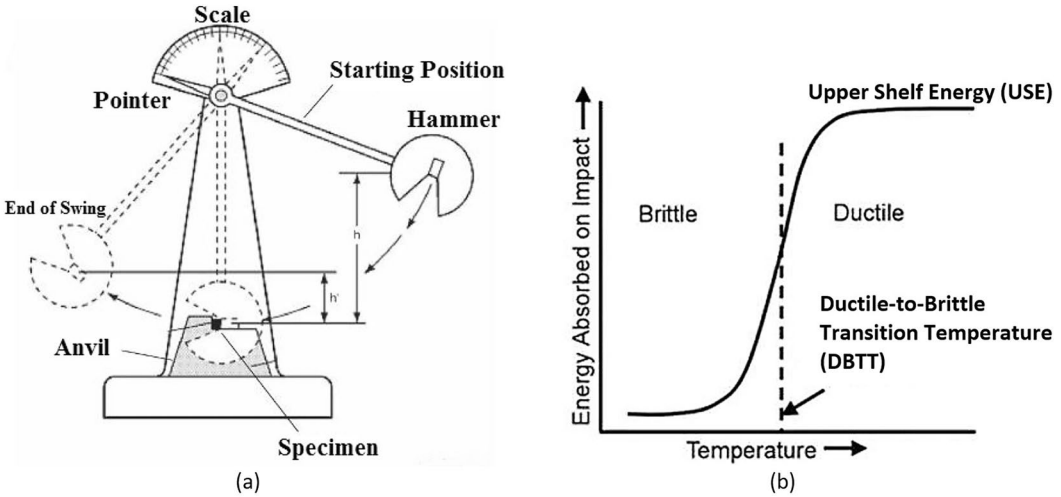


**Fig. 1** (**a**) Illustration of Charpy impact test setup[166]; (**b**) Ductile-to-brittle transition curve[167].

absorbed by the material during fracture is determined by measuring the height to which the pendulum swings after breaking the specimen. The absorbed energy reflects the material's ability to resist impact and deformation.

The most common testing approach standardized by ASTM E23[37] involves conducting Charpy V-notch tests at various temperatures. The measured values of impact energy plotted versus temperature are used to establish a pattern of energy absorption, referred to as the ductile-to-brittle transition (DBT) curves. A typical DBT curve is depicted in Fig. 1b and consists of three regions: an upper shelf region with high, nearly constant impact energy, a transition region characterized by a steep decrease in energy absorption, and a lower shelf region with low, nearly constant impact energy. The upper shelf region corresponds to ductile fracture behavior, whereas the lower shelf region corresponds to brittle fracture behavior. Due to inherent experimental variations, a model from the family of logistic sigmoid functions is typically fitted to the collected data of impact energies at various temperatures to obtain the DBT curve. E.g., a curve fitting with a hyperbolic tangent function is commonly adopted in many related studies.

Two key material features extracted from DBT curves are the upper shelf energy (USE) and the ductile-to-brittle transition temperature (DBTT) (shown in Fig. 1b). USE represents the energy absorbed in the ductile region, while DBTT is the temperature that marks the transition from high energy absorption to low energy absorption. These properties are essential for assessing material performance under varying conditions and identifying the material's suitability for specific operating conditions. Although the V-notch test is the most commonly used variation of the Charpy impact test, other variants with different notch shapes (e.g., U-notch) or without a notch are also employed for some applications.

**Specimen size effect.** Standards for Charpy impact testing have been developed by various organizations, and include ASTM E23[37], ISO 148-2[38], GB/T 229[39], and EN 10045-1[40]. These standards typically follow a full-sized Charpy specimen with length, thickness, and width dimensions of $55 \times 10 \times 10$ mm, a notch depth of 2 mm, a notch angle of 45°, and a notch root radius of 0.25 mm (ASTM E23). Sub-sized specimens with reduced thickness, such as 6.67 mm (2/3-size), 5 mm (1/2-size), and 2.5 mm (1/4-size), have been used for cases where specimens with full-size thickness cannot be extracted. Related studies have also used specimens that have reduced thickness, width, length, and notch dimensions, and are commonly referred to as miniature specimens. Historically, early Charpy standards did not account for sub-sized specimens. However, contemporary standards are being increasingly developed to standardize the use of sub-sized specimens for future testing.

As with most mechanical testing methods, specimen size has a significant influence on the measured mechanical properties of materials. In tensile testing, for instance, it is well-documented that reducing specimen dimensions often results in decreased ductility and increased strength[41–43]. Similar size effects are observed in Charpy V-notch tests, where changes in specimen dimensions impact USE and DBTT, with smaller specimens tending to exhibit lower USE and DBTT values[43,44]. Additionally, prior studies reported that while USE is primarily influenced by specimen thickness and ligament size, it shows minimal sensitivity to notch geometry. Conversely, DBTT is strongly affected by notch geometry, particularly by variations in notch depth and root radius[11,12].

Significant research efforts on understanding the specimen size effect have been dedicated in recent decades. Numerous studies have proposed methods to correlate the results of sub-sized Charpy V-notch specimens and full-sized specimens. These approaches aim to address the inherent difficulties in comparing mechanical property data across varying specimen sizes. The following sections present an overview of methods for correlation of USE and DBTT for sub-sized specimens.

**Correlation of Upper Shelf Energy.** Analytical methods for correlation of USE between sub-sized and full-sized Charpy specimens aim to establish relationships that account for the differences in specimen

| Authors | Methodology | Explanation |
|---|---|---|
| Lucas *et al.*[46] | $USE/B(W-A)^2$ | Normalization |
| Corwin *et al.*[47] | $USE/(B(W-A))^{3/2}$ | Normalization |
| Louden *et al.*[48] | $USE \cdot LK_t/B(W-A)^2$ | Normalization with stress concentration factor |
| Kayano *et al.*[49] | $USE \cdot K_t^{'}/(B(W-A))^{3/2}$ | Normalization with modified stress concentration factor |
| Kumar *et al.*[51] | $\Delta USE + USE_p$ | Sum of crack initiation and crack propagation energy |
| Sokolov *et al.*[52] | $USE(NF_{brittle}(1-S) + NF_{ductile}S)$ | Empirical sum of ductile fracture and brittle fracture |
| Uehira *et al.*[53] | $USE/m(Bb)^n$ | Empirical power-law correlation |
| Wallin[54] | $USE\frac{B}{10}\left[1-\left(0.5exp\left(0.11\frac{U_f}{B}-4.9\right)\right)/\left(1+exp\left(0.11\frac{U_f}{B}-4.9\right)\right)\right]$ | Empirical exponential correlation |

**Table 2.** Analytical methods for correlation of USE between sub-sized and full-sized Charpy specimens.

dimensions and geometry to achieve comparability of test results. Common correlation methods for USE are summarized in Table 2.

Several works introduced normalization factors that scale the USE of sub-sized specimens to approximate the USE of corresponding full-sized specimens manufactured from the same material and tested under the same conditions. Lucas *et al.*[45,46] proposed a normalization factor based on the fracture volume of the Charpy V-Noth specimen $B(W-A)^2$, where $B$ denotes the specimen thickness, $W$ is the width, and $A$ denotes the notch depth. The difference $W-A$ is the ligament size located under the notch. A modification of this method was proposed by Corwin *et al.*[13,47], where the fracture volume is calculated using $(B(W-A))^{3/2}$. The authors reported an adequate match of this method for ductile materials with USE greater than 150 [J].

The shortcoming of these methods is that they do not account for important factors such as the notch geometry or length of the specimen, which causes inconsistencies in the correlated values. Louden *et al.*[48] introduced a normalization factor $LK_t/B(W-A)^2$, which incorporates the specimen span $L$ and the stress concentration factor $K_t$ at the notch root. This approach produced an improved correlation for brittle materials with USE less than 100 [J]. Kayano *et al.*[49] further expanded this method by introducing a modified stress concentration factor $K_t^{'}$ calculated based on the notch angle.

Rosinski *et al.*[50] reported that the above methods are inappropriate for correlating Charpy test results for irradiated materials with USE above 200 [J] before irradiation. Consequently, Kumar *et al.*[44,51] proposed a method that divides USE into two components: the energy required to initiate a crack ($\Delta USE$), and the energy required to propagate the crack ($USE_p$). To calculate the correlated USE, the authors performed testing with both notched and precracked specimens to determine $\Delta USE$ and $USE_p$.

Sokolov *et al.*[52] developed a correlation method that considers the contributions of both brittle and ductile fractures to the change in impact energy. The proposed method employs normalization factors $NF_{brittle}$ and $NF_{ductile}$ that are empirically calculated based on the ratio of fracture surface for full-sized and sub-sized specimens, and $S$ is the percent of shear fracture on the fracture surface.

Another empirical correlation method was proposed by Uehira *et al.*[53], which employs a power-law relationship for the size effect defined as $USE/m(Bb)^n$, where the coefficients $m$ and $n$ and determined empirically using USE values for corresponding full-size specimens. Wallin *et al.*[21,54,55] developed the correlation method shown in Table 2, based on empirical observation that the fracture energy for 100% shear fracture is about half the energy for normal ductile tearing. The proposed method applies normalization of the USE by the thickness $B$ and fits a hyperbolic tangent function that starts at 1 and ends at 0.5.

While each of the proposed correlation approaches has unique strengths, they also have inherent limitations. The methods based on normalization by scaling factors are generally simplistic and unsuitable for general application across specimen geometries and materials. Conversely, other methods are excessively complex, relying on test-specific variables or assumptions, which compromise their reliability. Furthermore, some methods require additional experiments with precracked specimens or rely on empirical data to determine constants or parameters in the proposed models. Conclusively, the development of robust correlation methods that simultaneously account for material properties, specimen treatment, or testing parameters is still an open research problem.

## Correlation of Ductile-to-Brittle Transition Temperature

Analogously, studies in the published literature have proposed methods for the correlation of DBTT between sub-sized and full-sized test samples. Table 3 lists common DBTT correlation methods.

Conventional correlation techniques apply a constant temperature shift between the full-sized and sub-sized samples[9,43,52,56]. The temperature shift is determined empirically and it generally varies with the differences in specimen dimensions. For instance, Towers[52] recommended the following constant $0.7(10-B)^2$, Wallin *et el.*[54] proposed the constant $51.4 \cdot \ln(2B/10^{0.25}-1)$, and Lucon *et al.*[38] proposed $92.7-14.34 \cdot \ln(B \cdot (W-A)^2)$. This approach is the most basic technique to estimate the correlated DBTT.

Louden *et al.*[48] proposed a normalization factor for DBTT correlation given as $(2B(W-A)^2)/K_t 3P_m L$, where $K_t$ is the stress concentration factor, $P_m$ denotes the maximum load during a Charpy test, and the other parameters are as defined in the previous section. Kayano *et al.*[49] observed that using a normalization factor of $K_t^{'1/2}$ achieves adequate correlation for sub-sized specimens.

| Authors | Methodology | Explanation |
|---|---|---|
| Towers[165] | $DBTT + 0.7(10 - B)^2$ | Temperature shift of a constant |
| Wallin *et al.*[54] | $DBTT - 51.4 \cdot \ln(2B/10^{0.25} - 1)$ | Temperature shift of a constant |
| Lucon *et al.*[43] | $DBTT + 92.7 - 14.34 \cdot \ln(B \cdot (W - A)^2)$ | Temperature shift of a constant |
| Louden *et al.*[48] | $DBTT \cdot (2B(W - A)^2)/K_t 3P_m L$ | Normalization with stress concentration factor |
| Kayano *et al.*[49] | $DBTT/K_t^{'1/2}$ | Normalization with modified stress concentration factor |
| Kurishita *et al.*[12] | If $(A/\rho) \sim 15 \rightarrow DBTT$ | Using notch depth to root radius ratio |
| Uehira *et al.*[53] | $DBTT/(115(\log_{10} BK_t) - 158)$ | Empirical correlation |

**Table 3.** Analytical methods for correlation of DBTT between sub-sized and full-sized Charpy specimens.

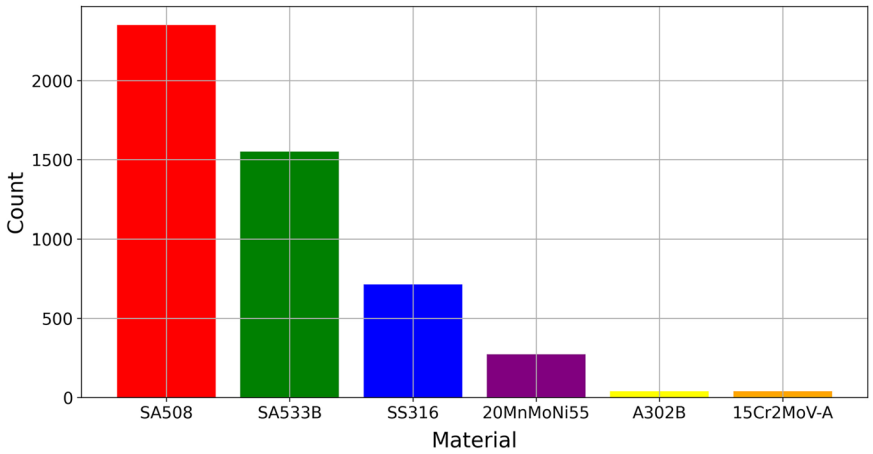


**Fig. 2** Histogram of the material class distribution.

Kurishita *et al.*[12] introduced a correlation based on the ratio of the notch depth $A$ to notch root radius $\rho$. When the ratio $A/\rho$ is approximately 15, the authors reported that DBTT of sub-sized specimens is approximately equal to DBTT for the corresponding full-sized specimens.

Uehira *et al.*[53] developed an empirical method that employs a logarithmic relationship including the sample thickness $B$ and stress concentration factor $K_t$.

Similar to the correlation methods for USE, the analytical methods for DBTT correlation are typically material and condition-specific and require calculation of empirical constants or parameters in order to be applicable to specific scenarios.

**Data acquisition.** We conducted the literature search primarily using Google Scholar with the query terms "Charpy impact test", "sub-sized Charpy", "SA533B Charpy Impact", "A533B Charpy Impact", "SA302 Charpy Impact", "A302 Charpy Impact", "20MnMoNi55 Charpy Impact", "SS316 Charpy Impact", and "toughness test". To address potentially missed results, additional search engines, including Google search and Bing search, were employed. This process resulted in 150 identified peer-reviewed publications containing potentially relevant data.

The next step included further analysis and refinement of the identified publications, based on inclusion criteria related to the specimen chemical composition, manufacturing treatment, irradiation conditions, mechanical properties, impact toughness energy, and test temperature. We considered publications that contain Charpy impact test results for RPV steels with a focus on the following steels: SA508, SA53B, 20MnMoNi55, and A302B. In addition, we collected data for Stainless Steel 316, due to its role as nuclear structural material. We collected Charpy test records for both sub-sized and full-sized specimens. Papers lacking the above information were excluded from further analysis, resulting in a final dataset based on 109 publications[7,8,10,57–162].

In the publications that presented the data in tabular format, we extracted the test records and stored them in a spreadsheet. A significant portion of the Charpy impact test data was presented in graphical form in the publications. We used the WebPlotDigitizer software[163] to manually extract data points from graphs and plots. All extracted data were compiled into a spreadsheet for further analysis, resulting in 4,961 Charpy impact test records in total.

**Data post-processing.** To ensure uniformity in the dataset, our team performed post-processing to standardize units and resolve inconsistencies. As many publications reported measurements in varying units, all values for the columns were converted to a single standard unit. For instance, temperatures reported in Fahrenheit or Kelvin degrees were converted to Celsius degrees. Additionally, material compositions often included the term

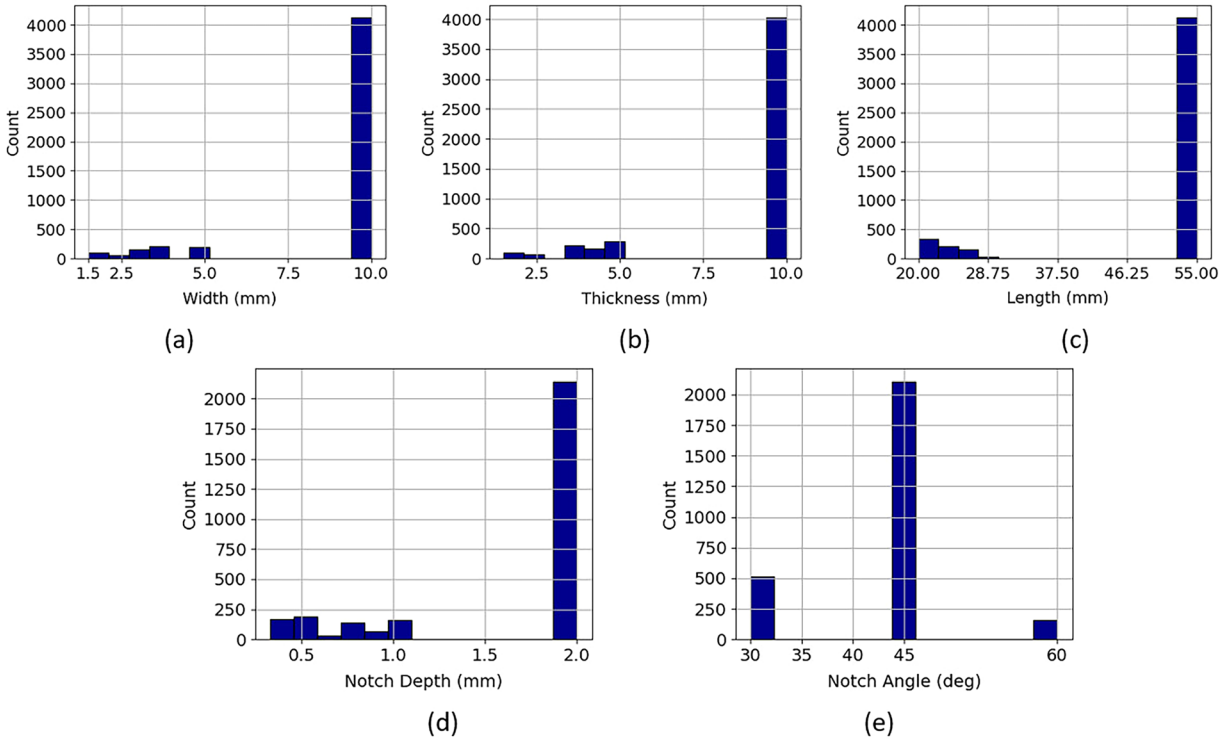


**Fig. 3** Histograms of specimen dimensions: (**a**) width, (**b**) thickness, (**c**) length, (**d**) notch depth, (**e**) notch angle.

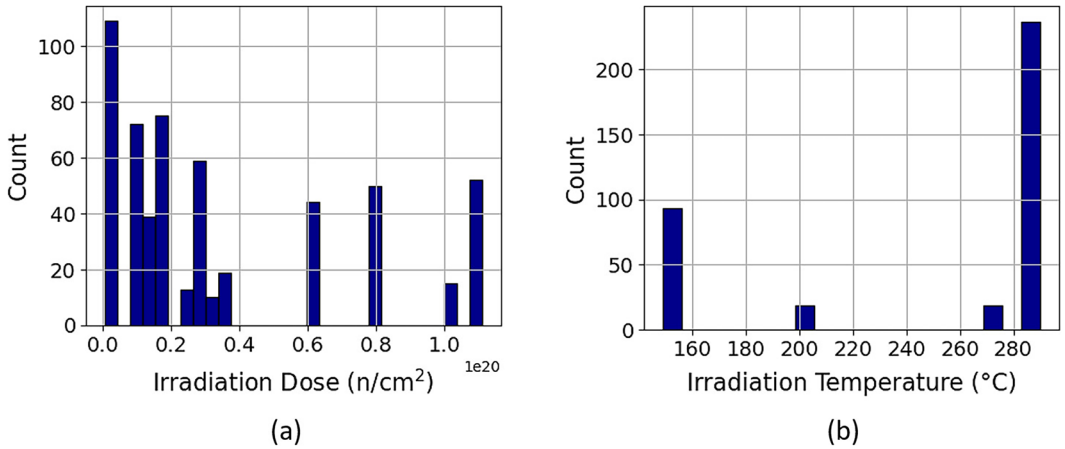


**Fig. 4** Histograms of irradiation conditions: (**a**) irradiation dose, (**b**) irradiation temperature.

"balance" for primary elements, such as Iron (Fe) in steels. This was remedied by subtracting the weight percentages (wt.%) of all other alloying elements to calculate the weight percentage of the primary element. Following post-processing, all values were standardized and recorded under consistent units to ensure compatibility and reliability for subsequent analysis.

**Data distribution.** The histogram of the distribution of specimens' materials in the dataset is shown in Fig. 2. The most common materials are SA508 and SA533B, followed by SS316, 20MnMoNi55, A302B, and 15Cr2MoV-A. The distributions of specimens' dimensions are shown in Fig. 3, where full-sized specimens have thickness and width of 10 mm and length of 55 mm, while sub-sized specimens have thickness and width ranging from 1.5 to 5 mm, and lengths between 20 and 27.5 mm. In addition, Fig. 3 also shows the histograms for the notch depth and notch angle. Figure 4 presents histograms of the irradiation dose and temperature for the irradiated specimens in the dataset. Figure 5 presents plots of the distributions of USE and DBTT in the dataset.

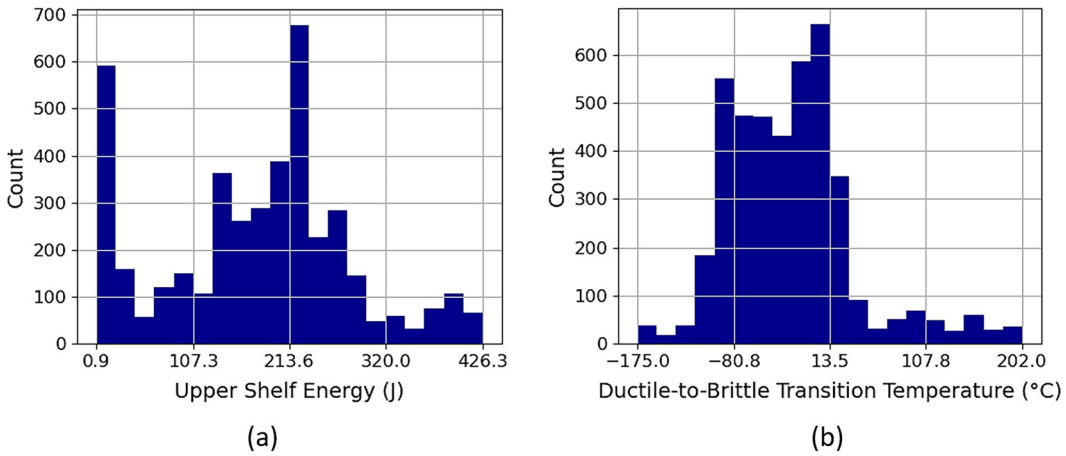


**Fig. 5** Histograms of Charpy parameters: (**a**) Upper Shelf Energy, (**b**) Ductile-to-Brittle Transition Temperature.

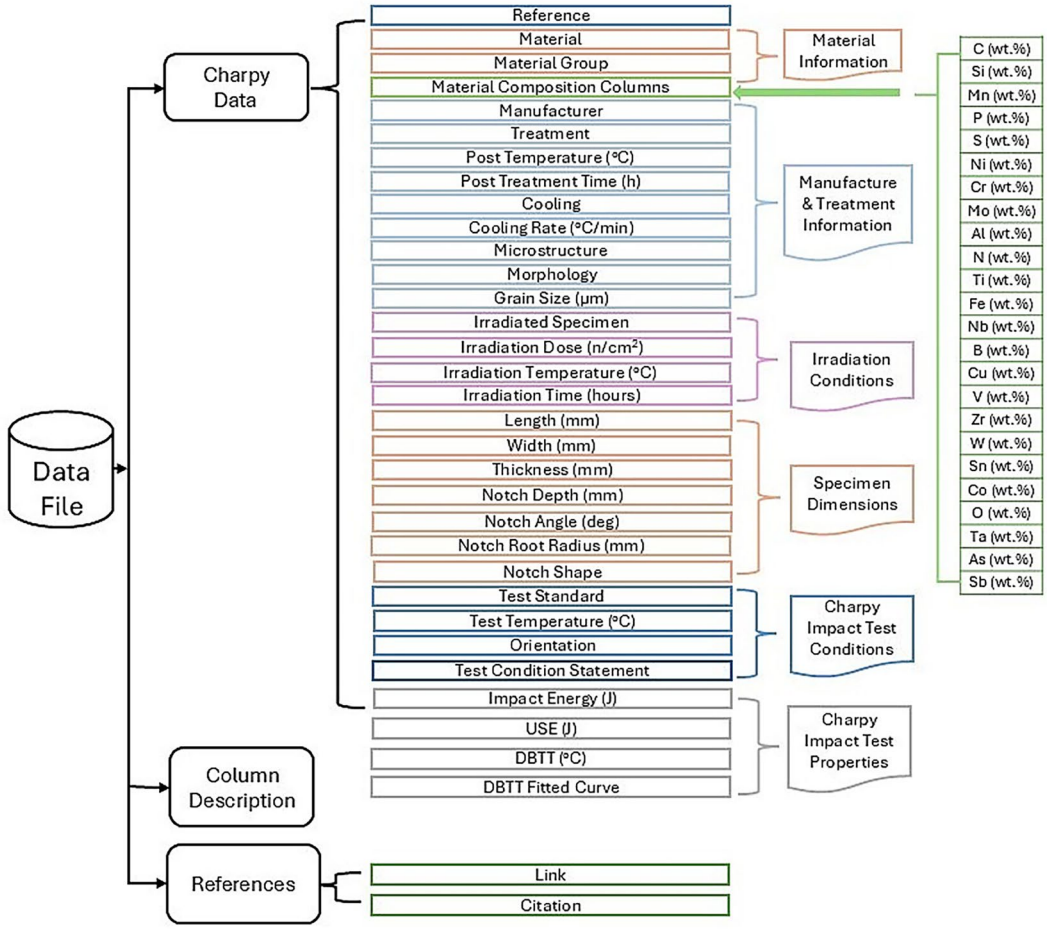


**Fig. 6** Organization of the dataset by columns and data categories.

## Data Records

The dataset is available at the Materials Cloud Archive[164]. The extracted data are stored in a spreadsheet format. Figure 6 provides a schematic representation of the dataset's structure and organization. The rows in the dataset contain retrieved data for individual Charpy impact tests. The dataset consists of 55 columns, categorized into the following groups: reference, material information, manufacturing and treatment information, irradiation conditions, specimen dimensions, Charpy test conditions, and Charpy properties. The worksheet includes a

"References" worksheet listing the publications from which the data was extracted, and a "Column Description" worksheet providing descriptions of the columns in the dataset.

The reference column contains the ID number corresponding to the publications in the References worksheet. The material information columns contain the name of the material for the test specimen and the chemical compositions. The manufacturing and treatment information columns provide important information related to the applied specimen treatment method, treatment time and temperature, cooling methods, microstructure, grain size, and morphology. The specimen irradiation conditions are important for nuclear applications of material, and include information for the irradiation dose, irradiation temperature, and time. The specimen dimensions and sizes are particularly important for this study and contain the testing standard, length, width, thickness, notch depth, notch angle, and notch root radius. The Charpy test conditions columns list the test temperature, test geometry, and specimen orientation. The Charpy properties columns provide the measured value for the impact energy and the estimated values for USE and DBTT.

## Usage Notes

It is important to note that a common challenge in compiling literature data is incomplete reporting and gaps in the provided information. Not all publications provide comprehensive information needed to populate all columns. Parameters such as microstructure, treatment details, or grain size are absent in some references, leading to gaps or blank entries in the worksheet. These limitations require a cautious interpretation of the data. In addition, potential errors can result from the data extraction procedure from publication graphs. As mitigation strategies, we ensured that the graph axes were calibrated carefully and that extraction procedures were consistent, and whenever feasible, extracted data points were cross validated with accessible tabular values in order to lessen these impacts. Despite these challenges, the dataset can serve as a valuable resource for validation and analysis of Charpy impact tests.

## Technical Validation

The collected data from the literature of Charpy impact tests underwent a rigorous process of review and validation by material science experts. The goal was to ensure the accuracy and reliability of the retrieved data, focusing on verifying features such as material composition, standardization of names and terms related to heat treatments and manufacturing methods, and validation that testing procedures are accurately extracted. Particular emphasis was placed on verifying specimen size information to ensure consistency and applicability to the study's objectives. The technical experts also verified the consistency of data conversion to standardized units of measurement.

Furthermore, statistical analyses were conducted and data visualizations were applied to identify and assess outliers within the dataset. Potential outliers were examined and either validated as legitimate data points or excluded based on deviation from established norms. Comprehensive technical validation ensured that the dataset is reliable, robust, and suitable for subsequent analysis or modeling.

## Code availability

Sample code in Python and Jupyter Notebooks for loading the dataset and analysis of the results are available at the following link: https://github.com/avakanski/Charpy-Impact-Test-Dataset/blob/main/Sample_Code.ipynb.

Received: 30 December 2024; Accepted: 13 March 2025;
Published online: 01 April 2025

## References

1. Gurovich, B. A. *et al*. Fine structure behaviour of VVER-1000 RPV materials under irradiation. *Journal of Nuclear Materials*, **389**(3), 490–496, https://doi.org/10.1016/j.jnucmat (2009).
2. Wright, R. N., Wright, J. K., Sham, T. L., Nanstad, R., Ren, W. *Next generation nuclear plant reactor pressure vessel materials research and development plan* (Report No. INL/EXT-**08**-14108). Idaho National Laboratory. (2008).
3. Kornecki, K. & Wise, C. F. The role of advanced nuclear reactors and fuel cycles in a future energy system. *PNAS Nexus* **3**(2), 1–7, https://doi.org/10.1093/pnasnexus/pgae030 (2024).
4. Liu, Z., Yang, B., Tian, L. & Zhang, F. Development and outlook of advanced nuclear energy technology. *Energy Strategy Reviews* **34**, 100630, https://doi.org/10.1016/j.esr.2021.100630 (2021).
5. Gussev, M. N., Howard, R. H., Terrani, K. A., Field, K. G. Sub-size tensile specimen design for in-reactor irradiation and post-irradiation testing. *Nuclear Engineering and Design*, **320**, 298–308. https://doi.org/10.1016/j.nucengdes (2017).
6. Kolhatkar, A. *et al*. Development and Standardization of Ultra Sub-size Tensile Specimen for Evaluation of Tensile Properties. (2016).
7. Schubert, L. E., Kumar, A. S., Rosinki, S. T. & Hamilton, M. L. Effect of specimen size on the impact properties of neutron irradiated A533B steel. *Journal of Nuclear Materials* **225**, 231–237, https://doi.org/10.1016/0022-3115(95)00052-6 (1995).
8. Kim, B. J., Mitsui, H., Kasada, R. & Kimura, A. Evaluation of impact properties of weld joint of reactor pressure vessel steels with the use of miniaturized specimens. *Journal of Nuclear Science and Technology* **49**, 618–631, https://doi.org/10.1080/00223131.2012.687235 (2012).
9. Alexander, D. J. & Klueh, R. L. Specimen size effects in Charpy impact testing. *ASTM Special Technical Publication* **1072**, 179–191, https://doi.org/10.1520/STP24145S (1990).
10. Dohi, K., Soneda, N., Onchi, T. & Matsui, H. Correlation between subsize and full-size Charpy impact properties of neutron-irradiated reactor pressure vessel steels. *ASTM Special Technical Publication* **1405**, 137–150, https://doi.org/10.1520/STP10818S (2002).
11. Kurishita, H., Kayano, H., Narui, M. & Yamazaki, M. Current status of small specimen technology in Charpy impact testing. *Journal of Nuclear Materials* **212–215**, 1682–1687, https://doi.org/10.1016/0022-3115(94)91113-4 (1994).
12. Kurishita, H. *et al*. Effects of V-notch dimensions on Charpy impact test results for differently sized miniature specimens of ferritic steel. *Materials Transactions, JIM* **34**(11), 1042–1052, https://doi.org/10.2320/matertrans1989.34.1042 (1993).

13. Corwin, W. R. & Houghland, A. M. Effect of specimen size and material condition on the Charpy impact properties of 9Cr-1Mo-V-Nb steel. *ASTM Special Technical Publication* **888**, 325–338, https://doi.org/10.1520/STP33014S (1986).
14. Camin, B. & Gille, M. The effect of specimen size and test procedure on the creep behavior of ME21 magnesium alloy. *Crystals* **11**(8), 918, https://doi.org/10.3390/cryst11080918 (2021).
15. Yu, B. *et al*. Application of small specimen test technique to evaluate creep behavior of austenitic stainless steel. *Materials*, **12**(2541). https://doi.org/10.3390/ma12162541 (2019).
16. Zvirko, O. *et al*. Specimen size effect on the tensile properties of rolled steel of long-term-operated portal crane. *Materials*, **16**(3017). https://doi.org/10.3390/ma16083017 (2023).
17. Han, L., Reynolds, N., Dargue, I. & Williams, G. The effect of specimen dimensions on obtained tensile properties of sheet metals. *Key Engineering Materials* **410-411**, 481–491 (2009).
18. Reer, J. R., Jang, D. & Gu, X. W. Exploring deformation mechanisms in nanostructured materials. *JOM* **64**(10), 1241–1252, https://doi.org/10.1007/s11837-012-0438-6 (2012).
19. Hurst, R. C., Matocha, K. A renaissance in the use of the small punch testing technique. In *Pressure Vessels and Piping Conference* (Vol. 56932, V01BT01A048). American Society of Mechanical Engineers, West Conshohocken, PA. https://doi.org/10.1115/PVP2015-45095 (2015).
20. Suzuki, K., Jitsukawa, S., Okubo, N. & Takada, F. Intensely irradiated steel components: Plastic and fracture properties, and a new concept of structural design criteria for assuring the structural integrity. *Nuclear Engineering and Design* **240**(6), 1290–1305, https://doi.org/10.1016/j.nucengdes.2010.02.031 (2010).
21. Wallin, K., Karjalainen-Roikonen, P. & Suikkanen, P. *Sub-sized CVN specimen conversion methodology* (Report No. INL/EXT-08-14108). *Procedia Structural Integrity* **2**, 3735–3742, https://doi.org/10.1016/j.prostr.2016.06.464 (2016).
22. Cicero, S. *et al*. Fracture mechanics testing of irradiated RPV steels by means of sub-sized specimens: FRACTESUS project. *Procedia Structural Integrity* **28**, 61–66, https://doi.org/10.1016/j.prostr.2020.10.008 (2020).
23. ASTM International. *ASTM* A370 / *ASME SA-370: Standard test methods and definitions for mechanical testing of steel products*. ASTM International. https://doi.org/10.1520/A0370-16 (2016).
24. British Standards Institution. BS **7910:**2019 - Guide to methods for assessing the acceptability of flaws in metallic structures. BSI Standards Limited. ISBN: 9780580520860.
25. American Petroleum Institute. (1998). *Piping Inspection Code: Inspection, Repair, Alteration, and Rerating of In-Service Piping Systems* (API **57**0, 2nd ed.). Retrieved from https://inldigitallibrary.inl.gov/sites/sti/sti/4215156.pdf (2019).
26. Konopik, P., Dżugan, J., Bucki, T., Rzepa, S. Correlation between standard Charpy and sub-size Charpy test results of selected steels in upper shelf region. *4th International Conference Recent Trends in Structural Materials*. https://doi.org/10.1088/1757-899X/179/1/012039 (2017).
27. Schmidt, J., Marques, M. R. G., Botti, S., Marques, M. A. L. Recent advances and applications of machine learning in solid-state materials science. *npj Computational Materials, 5*(1), **83**. https://doi.org/10.1038/s41524-019-0221-0 (2019).
28. Akbari, P., Zamani, M. & Mostafaei, A. Machine learning prediction of mechanical properties in metal additive manufacturing. *Additive Manufacturing* **91**, 104320, https://doi.org/10.1016/j.addma.2024.104320 (2024).
29. Stoll, A., Benner, P. Machine learning for material characterization with an application for predicting mechanical properties. *GAMM-Mitteilungen*, **44**(1). https://doi.org/10.1002/gamm.202100003 (2021).
30. Ahmedabadi, P. M. Comparison of mathematical and supervised machine-learning models for ductile-to-brittle transition in bcc alloys. *Materials Research Express* **11**, 076506, https://doi.org/10.1088/2053-1591/ad5cd8 (2024).
31. Jacobs, R., Yamamoto, T., Odette, G. R. & Morgan, D. Predictions and uncertainty estimates of reactor pressure vessel steel embrittlement using machine learning. *Materials & Design* **236**, 112491, https://doi.org/10.1016/j.matdes.2023.112491 (2023).
32. Mathew, J. *et al*. Reactor pressure vessel embrittlement: Insights from neural network modelling. *Journal of Nuclear Materials* **502**, 311–322, https://doi.org/10.1016/j.jnucmat.2018.02.027 (2018).
33. Morgan, D. *et al*. Machine learning in nuclear materials research. *Current Opinion in Solid State and Materials Science* **26**, 100975, https://doi.org/10.1016/j.cossms.2021.100975 (2022).
34. Odette, G. R., Yamamoto, T., Williams, T. J., Nanstad, R. K. & English, C. A. On the history and status of reactor pressure vessel steel ductile to brittle transition temperature shift prediction models. *Journal of Nuclear Materials* **526**, 151863, https://doi.org/10.1016/j.jnucmat.2019.151863 (2019).
35. Odette, G. R. *et al*. The UCSB IVAR, ATR-2, and BR2 irradiation experiments and the RPV steel hardening database used in recent machine learning studies. University of California, Santa Barbara. (2023).
36. Saba, N., Jawaid, M., Sultan, M. T. H. An overview of mechanical and physical testing of composite materials. In *Mechanical and Physical Testing of Biocomposites, Fibre-Reinforced Composites and Hybrid Composites* (pp. 1–12). Elsevier. https://doi.org/10.1016/B978-0-08-102292-4.00001-1 (2019).
37. ASTM International. *ASTM E23-23: Standard Test Methods for Notched Bar Impact Testing of Metallic Materials*. ASTM International (2023).
38. International Organization for Standardization. *ISO* **148***-2:2016: Metallic materials—Charpy pendulum impact test—Part 2: Verification of testing machines*. Geneva, Switzerland: ISO. (2016).
39. Zheng. W. GB/T **229**-2020 PDF in English. www.ChineseStandard.net. (2021).
40. European Committee for Standardization. EN **10045**-1: *Metallic materials – Charpy impact test – Part 1: Test method*. Brussels: CEN. (1990).
41. Strnadel, B. & Brumek JEffect Of Tensile Test Specimen Size On Ductility Of R7t Steel. (2013).
42. Yuan, W. J., Zhang, Z. L., Su, Y. J., Qiao, L. J. & Chu, W. Y. Influence of specimen thickness with rectangular cross-section on the tensile properties of structural steels. *Materials Science and Engineering: A* **532**, 601–605, https://doi.org/10.1016/j.msea (2012). 2011.11.021.
43. Lucon, E., McCowan, C. N., Santoyo, R. L. Impact characterization of line pipe steels by means of standard, sub-size, and miniaturized Charpy specimens. *NIST Technical Note 1865*. https://doi.org/10.6028/NIST.TN.1865 (2015).
44. Kumar, A. S., Louden, B. S., Garner, F. A. & Hamilton, M. L. Recent improvements in size effects correlations for DBTT and upper shelf energy of ferritic steels. *ASTM Special Technical Publication* **1204**, 69–84 (1993).
45. Lucas, G. E., Odette, G. R., Sheckherd, J. W., McConnell, P. & Perrin, J. Subsized bend and Charpy V-notch specimens for irradiated testing. *ASTM Special Technical Publication* **888**, 369–387 (1986).
46. Lucas, G. E., Odette, G. R., Sheckherd, J. W. & Krishnadev, M. R. Recent progress in subsized Charpy impact specimen testing for fusion reactor materials development. *Fusion Technology* **10**, 728–733, https://doi.org/10.13182/FST86-A24827 (1986).
47. Corwin, W. R., Klueh, R. L. & Vitek, J. M. Effect of specimen size and nickel content on the impact properties of 12 Cr-1 MoVW ferritic steel. *Journal of Nuclear Materials* **122**, 343–348, https://doi.org/10.1016/0022-3115(84)90622-6 (1984).
48. Louden, B. S., Kumar, A. S., Garner, F. A., Hamilton, M. L. & Hu, W. L. The influence of specimen size on Charpy impact testing of unirradiated HT-9. *Journal of Nuclear Materials* **155–157**, 662–667, https://doi.org/10.1016/0022-3115(88)90391-1 (1988).
49. Kayano, H. *et al*. Charpy impact testing using miniature specimens and its application to the study of irradiation behavior of low-activation ferritic steels. *Journal of Nuclear Materials* **179–181**, 425–428, https://doi.org/10.1016/0022-3115(91)90115-N (1991).
50. Rosinski, S. T., Kumar, A. S., Cannon, N. S. & Hamilton, M. L. Application of subsize specimens in nuclear plant life extension. *ASTM Special Technical Publication* **1204**, 353–368, https://www.osti.gov/biblio/10158146 (1993).

51. Kumar, A. S., Rosinski, S. T., Cannon, N. S. & Hamilton, M. L. Subsize specimen testing of a nuclear reactor pressure vessel material. *ASTM Special Technical Publication* **1175**, 1344–1352 (1994).
52. Sokolov, M. A. & Nanstad, R. K. On impact testing of subsize Charpy V-notch type specimens. *ASTM Special Technical Publication* **1325**, 437–467, https://doi.org/10.1520/STP16486S (1996).
53. Uehira, A. & Ukai, S. Empirical correlation of specimen size effects in Charpy impact properties of 11Cr-0.5Mo-2W, V, Nb ferritic-martensitic stainless steel. *Journal of Nuclear Science and Technology* **41**, 973–980, https://doi.org/10.3327/jnst.41.973 (2004).
54. Wallin, K. Upper shelf energy normalisation for sub-sized Charpy-V specimens. *International Journal of Pressure Vessels and Piping* **78**(7), 463–470, https://doi.org/10.1016/S0308-0161(01)00063-1 (2001).
55. Wallin, K. Sub-sized and miniature CVN specimen conversion methodology. *International Journal of Pressure Vessels and Piping* **183**, 1–10, https://doi.org/10.1016/j.ijpvp.2020.104080 (2020).
56. Amayev, A. D. *et al*. Use of subsize specimens for determination of radiation embrittlement of operating reactor pressure vessels. *ASTM Special Technical Publication* **1204**, 369–384, https://doi.org/10.1520/STP12746S (1993).
57. Server, W. L., Wullaert, R. A., Odette, G. R. & Oldfield, W. *Analysis of radiation embrittlement reference toughness curves* (Final report). United States. https://doi.org/10.2172/6609271 (1981).
58. Wullaert, R. A., Sheckherd, J. W. & Smith, R. W. Evaluation of the Maine Yankee reactor beltline materials. In F. Shober (Ed.), Irradiation effects on the microstructure and properties of metals. West Conshohocken, PA: ASTM International. https://doi.org/10.1520/STP38062S (1976).
59. Hiser, A. L. *Post-Irradiation Fracture Toughness Characterization of Four Lab-Melt Plates*. NUREG/CR-5216. Materials Engineering Associates, Inc., prepared for the U.S. Nuclear Regulatory Commission, Division of Engineering, Office of Nuclear Regulatory Research. https://doi.org/10.2172/6238942 (1989).
60. Kim, J. T., Kwon, H. K., Chang, H. S. & Park, Y. W. Improvement of impact toughness of the SA 508 class 3 steel for nuclear pressure vessel through steel-making and heat-treatment practices. *Nuclear Engineering and Design* **174**(1), 51–58, https://doi.org/10.1016/S0029-5493(97)00068-X (1997).
61. Logsdon, W. Dynamic Fracture Toughness of ASME SA508 Class 2a Base and Heat-Affected-Zone Material. *Elastic-Plastic Fracture*. https://doi.org/10.1520/stp35846s (1979).
62. Kim, J., Hong, S., Lee, T. & Kim, M. Estimation of Charpy index temperature of SA 508 Mn-Mo-Ni low alloy steels at 41J using small punch tests. *Proceedings of the ASME 2020 Pressure Vessels and Piping Conference: Volume 6: Materials and Fabrication*. V006T06A074. ASME. https://doi.org/10.1115/PVP2020-21360 (2020).
63. Kim, S., Lee, S., Im, Y. R. & others Effects of alloying elements on mechanical and fracture properties of base metals and simulated heat-affected zones of SA 508 steels. *Metallurgical and Materials Transactions A* **32**, 903–911, https://doi.org/10.1007/s11661-001-0347-8 (2001).
64. Kim, M.-C., Park, S.-G., Lee, K.-H. & Lee, B.-S. Comparison of fracture properties in SA508 Gr.3 and Gr.4N high strength low alloy steels for advanced pressure vessel materials. *International Journal of Pressure Vessels and Piping* **131**, 60–66, https://doi.org/10.1016/j.ijpvp.2015.04.010 (2015).
65. Lee, B. S., Kim, M. C., Yoon, J. H. & Hong, J. H. Characterization of high strength and high toughness Ni–Mo–Cr low alloy steels for nuclear application. *International Journal of Pressure Vessels and Piping* **87**(1), 74–80, https://doi.org/10.1016/j.ijpvp.2009.11.001 (2010).
66. Kim, M., Lee, K., Lee, B. & Kim, W. Mechanical properties of SA508 Gr.4N model alloys as a high strength RPV steel. *Proceedings of the ASME 2010 Pressure Vessels and Piping Division/K-PVP Conference*: Volume 9, Bellevue, Washington, USA, July 18–22, 2010, pp. 143–148. ASME. https://doi.org/10.1115/PVP2010-26002 (2010).
67. Yang, Z. *et al*. Effect of microstructure on the impact toughness and temper embrittlement of SA508Gr.4N steel for advanced pressure vessel materials. *Scientific Reports* **8**, 207, https://doi.org/10.1038/s41598-017-18434-3 (2018).
68. Ahn, Y.-S. *et al*. Application of intercritical heat treatment to improve toughness of SA508 Cl.3 reactor pressure vessel steel. *Nuclear Engineering and Design* **194**(2–3), 161–177, https://doi.org/10.1016/S0029-5493(99)00196-X (1999).
69. Lee, K.-H., Jhung, M. J., Kim, M.-C. & Lee, B.-S. Effects of tempering and PWHT on microstructures and mechanical properties of SA508 Gr.4N steel. *Nuclear Engineering and Technology* **46**(3), 413–422, https://doi.org/10.5516/NET.07.2013.088 (2014).
70. Park, S. G., Wee, D. M., Kim, M. C. & Lee, B. S. Effects of the phase fractions on the carbide morphologies, Charpy, and tensile properties in SA508 Gr4N high strength low alloy RPV steel. *Proceedings of the KNS Spring Meeting*, (pp. 1CD-ROM). Korea, Republic of: KNS. (2011).
71. Lee, Y. S., Kim, M. C. & Lee, B. S. Changes in Charpy impact properties with post weld heat treatment in the HAZ of SA508. *Transactions of the Korean Nuclear Society Autumn Meeting*, PyeongChang, Korea, October 25–26, 2007. (2007).
72. Kim, M. & Lee, B. Irradiation embrittlement behavior of SA508 Gr.4N RPV steel model alloy. *Proceedings of the ASME 2016 Pressure Vessels and Piping Conference*: Volume 6B: Materials and Fabrication, Vancouver, British Columbia, Canada, July 17–21, 2016, V06BT06A016. ASME. https://doi.org/10.1115/PVP2016-63446 (2016).
73. Park, S. G., Kim, M. C., Lee, B. S. & Wee, D. M. Evaluation of the microstructure and mechanical properties in SA508 Gr. 4N low alloy steel with a nickel and chromium contents variation. *Transactions of the Korean Nuclear Society Autumn Meeting*, PyeongChang, Korea, October 25–26. (2007).
74. Guo, W., Dong, S., Guo, W., Francis, J. A. & Li, L. Microstructure and mechanical characteristics of a laser welded joint in SA508 nuclear pressure vessel steel. *Materials Science and Engineering*: A, 625, 65–80, https://doi.org/10.1016/j.msea (2015).
75. Lee, K. H., Park, S. G., Kim, M. C., Lee, B. S. & Wee, D. M. Effects of alloying element contents on the toughness and transition behavior in the SA508 Gr. 4N Ni-Mo-Cr low alloy steels. *Transactions of the Korean Nuclear Society Spring Meeting*, Jeju, Korea, May 22. (2009).
76. Lee, K.-H., Park, S.-G., Kim, M.-C., Lee, B.-S. & Wee, D.-M. Characterization of transition behavior in SA508 Gr.4N Ni–Cr–Mo low alloy steels with microstructural alteration by Ni and Cr contents. *Materials Science and Engineering: A* **529**, 156–163, https://doi.org/10.1016/j.msea.2011.09.012 (2011).
77. Perrin, J. S., Fromm, E. O., Server, W. L. & McConnell, P. E. *Preparation of reconstituted Charpy V-notch impact specimens for generating pressure vessel steel fracture toughness data*. United States. https://www.osti.gov/biblio/5828458 (1982).
78. Hyun, S. M. *et al*. Effect of intercritical heat treatment on J-R fracture resistance of SA508 Gr.1A low-alloy steels. *Metals and Materials International* **28**, 2907–2918, https://doi.org/10.1007/s12540-022-01188-7 (2022).
79. Hong, S. *et al*. Effect of cooling rate on mechanical properties of SA508 Gr.1A steels for main steam line piping in nuclear power plants. *International Journal of Pressure Vessels and Piping* **191**, 104359, https://doi.org/10.1016/j.ijpvp.2021.104359 (2021).
80. Logsdon, W. Dynamic fracture toughness and fatigue crack growth rate properties of ASME SA508 CL 3 and SA508 CL 3a base and heat-affected-zone materials. *Journal of Testing and Evaluation*, **10**(4), 144–155. *ASTM International*. https://doi.org/10.1520/JTE11572J (1982).
81. Kim, J., Yang, B. & Kwon, H. The effects of intercritical heat treatment of the SA508 Grade 3 Class 1 steel before welding on the mechanical properties in its welded joint. *Proceedings of the ASME 2002 Pressure Vessels and Piping Conference*: Computational Weld Mechanics, Constraint, and Weld Fracture, Vancouver, BC, Canada, August 5–9, 2002, pp. 181–185. ASME. https://doi.org/10.1115/PVP2002-1122 (2002).
82. Kim, M.-C., Park, S.-G., Choi, K.-J. & Lee, B.-S. Effect of cooling rate on microstructures and mechanical properties in SA508 Gr4N high strength low alloy steel. *Transactions of the Korean Nuclear Society Spring Meeting*, Gwangju, Korea, May 30–31. (2013).

83. Park, S. G., Kim, M. C., Lee, B. S. & Wee, D. M. Effects of the chromium and molybdenum on precipitation behavior and mechanical properties in SA508 Gr. 4N low alloy steel. *Transactions of the Korean Nuclear Society Spring Meeting*, Gyeongju, Korea, May 29–30. (2008).
84. Park, S. G., Kim, M.-C., Lee, B. S. & Wee, D. M. Evaluation of the temper embrittlement in SA508 Gr. 4N low alloy steel with Ni, Cr contents variation. *Transactions of the Korean Nuclear Society Autumn Meeting*, Gyeongju, Korea, October 29–30. (2009).
85. Kim, M.-C., Park, S.-G., Lee, K.-H. & Lee, B.-S. High strength SA508 Gr.4N Ni-Cr-Mo low alloy steels for larger pressure vessels of the advanced nuclear power plant. *Transactions of the Korean Society of Pressure Vessels and Piping* **10**(1), 100–106, https://doi.org/10.20466/KPVP.2014.10.1.100 (2014).
86. Hyun, S.-M., Kim, M.-C., Hong, S., Kim, J. & Sohn, S. S. Effects of microalloying element addition on mechanical properties of SA508 Gr.1A low-alloy steels. *Nuclear Engineering and Technology*. https://doi.org/10.1016/j.net.2024.03.049 (2024).
87. Jeong, W. *et al*. Enhancement of strength and ductile-brittle transition temperature of SA508 Gr.3 low-alloy steel by controlling heat accumulation in laser powder-directed energy deposition. *Journal of Materials Science & Technology* **202**, 240–252, https://doi.org/10.1016/j.jmst.2024.02.042 (2024).
88. Hong, S., Hyun, S. M., Kim, J. M. & others Effect of Mo and V addition on microstructure and mechanical properties of SA508 Gr.1A steel for pipeline in nuclear power plants. *Metallurgical and Materials Transactions A* **53**, 1499–1511, https://doi.org/10.1007/s11661-022-06616-2 (2022).
89. Park, S. G., Kim, M.-C., Lee, B. S. & Wee, D. M. Study on the segregation behavior in SA508 Gr. 4N low alloy steel with Mn contents variation. *Transactions of the Korean Nuclear Society Spring Meeting*, Jeju, Korea, May 22. (2009).
90. Nanstad, R. K., Chen, X., Sokolov, M. A., Rabin, B. H. & Yang, Y. Master curve and J-R fracture toughness of SA508/SA533-B-1 weld and HAZ. *Proceedings of the ASME 2013 Pressure Vessels and Piping Conference*: Volume 6B: Materials and Fabrication, Paris, France, July 14–18, 2013, V06BT06A001. ASME. https://doi.org/10.1115/PVP2013-97033 (2013).
91. Lin, Y., Yang, W., Tong, Z., Zhang, C. & Ning, G. Charpy impact test on A508-3 steel after neutron irradiation. *Engineering Failure Analysis* **82**, 733–740, https://doi.org/10.1016/j.engfailanal.2017.06.032 (2017).
92. Zhou, Z., Huang, S., Hui, H. & Zhang, Y. Estimation of minimum design metal temperature by MDMT curve and correlations of Charpy impact and fracture toughness. *Journal of Pressure Vessel Technology* **142**(6), 061504, https://doi.org/10.1115/1.4046888 (2020).
93. Park, S. G., Kim, M.-C., Lee, B. S. & Wee, D. M. Comparison of the microstructure and segregation behavior between SA508 Gr.3 and SA508 Gr.4N high strength low alloy RPV steel. *Transactions of the Korean Nuclear Society Spring Meeting*, Pyeongchang, Korea, May 27–28. (2010).
94. Park, S.-G., Lee, K.-H., Min, K.-D., Kim, M.-C. & Lee, B.-S. Influence of the thermodynamic parameters on the temper embrittlement of SA508 Gr.4N Ni–Cr–Mo low alloy steel with variation of Ni, Cr and Mn contents. *Journal of Nuclear Materials* **426**(1–3), 1–8, https://doi.org/10.1016/j.jnucmat.2012.02.032 (2012).
95. Kim, B.-O. & Lee, O.-Y. The study of nuclear reactor pressure vessel steel SA508Gr.3 mechanical properties and temper-parameter. *Journal of the Korean Society for Heat Treatment* **25**(3), 121–125, https://doi.org/10.12656/JKSHT.2012.25.3.121 (2012).
96. Hong, S., Hyun, S. M., Kim, J. & others Effects of the alloy design and fabrication process on mechanical properties of Mo + V-added SA508 Gr.1A steel for main steam line piping in nuclear power plants. *Metals and Materials International* **29**, 693–704, https://doi.org/10.1007/s12540-022-01267-9 (2023).
97. El-Fadaly, M. S., ElSarrage, T. A., Eleiche, A. M. & Dahl, W. Fracture toughness of 20MnMoNi55 steel at different temperatures as affected by room-temperature pre-deformation. *Journal of Materials Processing Technology* **54**(1–4), 159–165, https://doi.org/10.1016/0924-0136(95)01936-7 (1995).
98. Bhowmik, S. *et al*. Estimation of fracture toughness of 20MnMoNi55 steel in the ductile to brittle transition region using master curve method. *Nuclear Engineering and Design* **241**(8), 2831–2838, https://doi.org/10.1016/j.nucengdes.2011.05.033 (2011).
99. Chaouadi, R. & Gérard, R. Development of a method for extracting fracture toughness from instrumented Charpy impact tests in the ductile and transition regimes. *Theoretical and Applied Fracture Mechanics* **115**, 103080, https://doi.org/10.1016/j.tafmec.2021.103080 (2021).
100. Chaouadi, R. & Puzzolante, J. L. Loading rate effect on ductile crack resistance of steels using precracked Charpy specimens. *International Journal of Pressure Vessels and Piping* **85**(11), 752–761, https://doi.org/10.1016/j.ijpvp.2008.08.004 (2008).
101. Bhowmik, S. *et al*. *Application of master curve methodology in the ductile to brittle transition region for the material 20MnMoNi55 steel*. (2011).
102. Gupta, C. Analysis of ductile-to-brittle transition characteristics of reactor pressure vessel steels. *Nuclear Technology* **209**(4), 560–581, https://doi.org/10.1080/00295450.2022.2143730 (2023).
103. Blauel, J. G., Hodulak, L., Hollstein, T. & Voss, B. Material characterization by J-R curves of a 20MnMoNi55 forging. *International Journal of Pressure Vessels and Piping* **17**(3), 139–162, https://doi.org/10.1016/0308-0161(84)90066-8 (1984).
104. Gupta, C., Singh, R. N. & Krishnan, M. *Mechanical properties of new generation CrMoV steel and comparison with selected western grade steels for reactor pressure vessel beltline applications using model functions* (BARC–2021/E/005). India. (2021).
105. Kim, B. J., Kasada, R. & Kimura, A. Effects of chemical composition on the impact properties of A533B steels. In *Materials Science Forum* (Vols. 654–656, pp. 2895–2898). Trans Tech Publications, Ltd. https://doi.org/10.4028/www.scientific.net/msf.654-656.2895 (2010).
106. Hawthorne, J. R. Postirradiation dynamic tear and Charpy-V performance of 12-in. thick A533-B steel plates and weld metal. *Nuclear Engineering and Design* **17**(1), 116–130, https://doi.org/10.1016/0029-5493(71)90044-6 (1971).
107. Tanguy, B., Besson, J., Piques, R. & Pineau, A. Ductile to brittle transition of an A508 steel characterized by Charpy impact test: Part I: Experimental results. *Engineering Fracture Mechanics* **72**(1), 49–72, https://doi.org/10.1016/j.engfracmech.2004.03.010 (2005).
108. Chaouadi, R., Van Eyken, J., Gérard, R., Lambrecht, M. & Uytdenhouwen, I. Effect of step cooling and P-segregation to grain boundaries on the tensile and fracture toughness properties of A533B plate and A508 forging steels. *Journal of Nuclear Materials* **550**, 152924, https://doi.org/10.1016/j.jnucmat.2021.152924 (2021).
109. Kumar, A. S., Schubert, L. E., Cannon, N. S. & Hamilton, M. L. Effect of neutron irradiation on the impact properties of A533B steel. In W. R. Corwin, W. L. Server & F. M. Haggag (Eds.), Small specimen test techniques and their application to nuclear reactor vessel thermal annealing and plant life extension *American Society for Testing and Materials*. (pp. 424-439). https://doi.org/10.2172/10191340 (1993).
110. Server, W. L., Norris, D. M., Jr. & Prado, M. E. *Ductile crack initiation in the Charpy V-notch test*. United States. https://www.osti.gov/biblio/6826263 (1978).
111. Murty, K. L., Shogan, R. P. & Bamford, W. H. Dynamic fracture toughness of irradiated A533 Grade B Class 1 pressure vessel steel. *Nuclear Technology* **64**(3), 268–274, https://doi.org/10.13182/NT84-A33356 (1984).
112. Nasreldin, A. M., Ibrahim, O. H. & Ghoneim, M. M. Effect of specimen size and notch geometry on the impact properties of the nuclear reactor pressure vessel steel A533 B. *Proceedings of the Sixth Arab Conference on the Peaceful Uses of Atomic Energy*, Vol. II: Scientific Presentation (Reactors, Materials, Fuel Cycles and Nuclear Safety), Egypt. (p. 626). https://inis.iaea.org/search/search.aspx?orig_q=RN:35095204 (2003).
113. Yuya, H., Kobayashi, R., Otomo, K., Yabuuchi, K. & Kimura, A. Microstructure and mechanical properties of HAZ of RPVS clad with duplex stainless steel. *Journal of Nuclear Materials* **545**, 152756, https://doi.org/10.1016/j.jnucmat.2020.152756 (2021).
114. Nguyen, L. T. H. *et al*. Charpy impact properties of hydrogen-exposed 316L stainless steel at ambient and cryogenic temperatures. *Metals* **9**(6), 625, https://doi.org/10.3390/met9060625 (2019).

115. Wang, S., Yang, K., Shan, Y. & Li, L. Plastic deformation and fracture behaviors of nitrogen-alloyed austenitic stainless steels. *Materials Science and Engineering: A* **490**(1–2), 95–104, https://doi.org/10.1016/j.msea.2008.01.015 (2008).
116. Kumar, A., Singh, B. & Sandhu, S. S. Effect of thermal aging on metallurgical, tensile and impact toughness performance of electron beam welded AISI 316 SS joints. *Fusion Engineering and Design* **159**, 111949, https://doi.org/10.1016/j.fusengdes.2020.111949 (2020).
117. Çalik, A. *et al*. Mechanical properties of boronized AISI 316, AISI 1040, AISI 1045, and AISI 4140 steels. *Acta Physica Polonica A* **115**, 694–698 (2009).
118. Wang, X. *et al*. Crystallographic orientation dependence of Charpy impact behaviours in stainless steel 316L fabricated by laser powder bed fusion. *Additive Manufacturing* **46**, 102104, https://doi.org/10.1016/j.addma.2021.102104 (2021).
119. Bunchoo, N., Wongpinkaew, K., Kukiatkulchai, E., Kaewkumsai, S. & Viyanit, E. Effects of thermal history on sensitization behavior and Charpy impact property of type 316L and 316 stainless steels for applications in a fired heater. *Engineering Failure Analysis* **141**, 106672, https://doi.org/10.1016/j.engfailanal.2022.106672 (2022).
120. Rodrigues, B. *et al*. *Evaluation of dynamic fracture mechanics in the AISI 316 stainless steel using instrumented Charpy impact testing*. (2007).
121. Sikka, V. K. *Effects of thermal aging on the mechanical properties of type 316 stainless steel - elevated-temperature properties*. United States. https://doi.org/10.2172/708800 (1982).
122. Nam, Y.-H., Park, J.-S., Baek, U.-B., Suh, J.-Y. & Nahm, S.-H. Low-temperature tensile and impact properties of hydrogen-charged high-manganese steel. *International Journal of Hydrogen Energy* **44**(13), 7000–7013, https://doi.org/10.1016/j.ijhydene.2019.01.065 (2019).
123. Byun, T. S. & Lach, T. G. *Mechanical properties of 304L and 316L austenitic stainless steels after thermal aging for 1500 hours* (PNNL-25854). Pacific Northwest National Laboratory, U.S. Department of Energy, Office of Nuclear Energy. (2016).
124. Kyffin, W., Gandy, D. & Burdett, B. A systematic study of the material performance of hot isostatically pressed type 316L stainless steel powder for the civil nuclear sector. *Proceedings of the 2018 26th International Conference on Nuclear Engineering*: Volume 2: Plant Systems, Structures, Components, and Materials; Risk Assessments and Management, London, England, July 22–26, 2018, V002T03A017. ASME. https://doi.org/10.1115/ICONE26-81438 (2018).
125. Gu, B. *et al*. Enhanced impact toughness of 316L stainless steel welded joint by ultrasonic impact. *Materials Today Communications* **39**, 109277, https://doi.org/10.1016/j.mtcomm.2024.109277 (2024).
126. Muster, W. J. & Elster, J. Low temperature embrittlement after ageing stainless steels. *Cryogenics* **30**(9), 799–802, https://doi.org/10.1016/0011-2275(90)90278-K (1990).
127. Byun, T. S., Collins, D. A., Lach, T. G. & Carter, E. L. Degradation of impact toughness in cast stainless steels during long-term thermal aging. *Journal of Nuclear Materials* **542**, 152524, https://doi.org/10.1016/j.jnucmat.2020.152524 (2020).
128. Tabrizi, T. R. *et al*. Comparing the effect of continuous and pulsed current in the GTAW process of AISI 316L stainless steel welded joint: Microstructural evolution, phase equilibrium, mechanical properties, and fracture mode. *Journal of Materials Research and Technology* **15**, 199–212, https://doi.org/10.1016/j.jmrt.2021.07.154 (2021).
129. Rautio, T., Jaskari, M., Keskitalo, M., Päkkilä, J. & Järvenpää, A. Fatigue strength and impact toughness dependence of powder bed fusion with laser beam-manufactured 316L stainless steel on orientation and layer thickness. *Journal of Laser Applications* **35**(4), 042062, https://doi.org/10.2351/7.0001113 (2023).
130. Afkhami, S., Dabiri, M., Piili, H. & Björk, T. Effects of manufacturing parameters and mechanical post-processing on stainless steel 316L processed by laser powder bed fusion. *Materials Science and Engineering: A* **802**, 140660, https://doi.org/10.1016/j.msea.2020.140660 (2021).
131. Wang, C., Lin, X., Wang, L., Zhang, S. & Huang, W. Cryogenic mechanical properties of 316L stainless steel fabricated by selective laser melting. *Materials Science and Engineering: A* **815**, 141317, https://doi.org/10.1016/j.msea.2021.141317 (2021).
132. Pitrmuc, Z. *et al*. Mechanical and microstructural anisotropy of laser powder bed fusion 316L stainless steel. *Materials* **15**(2), 551, https://doi.org/10.3390/ma15020551 (2022).
133. Miyahara, K., Bae, D.-S., Kimura, T. & Shimoide, Y. Phase instability and toughness change during high temperature exposure of various steels for the first wall structural materials of a fusion reactor. *Journal of Nuclear Materials* **226**(1–2), 92–103, https://doi.org/10.1016/0022-3115(95)00118-2 (1995).
134. AghaAli, I., Farzam, M., Golozar, M. A. & Danaee, I. The effect of repeated repair welding on mechanical and corrosion properties of stainless steel 316L. *Materials & Design* **54**, 331–341, https://doi.org/10.1016/j.matdes.2013.08.052 (2014).
135. Ogata, T. & Ishikawa, K. Effects of cold-rolling and Ni-equivalent on mechanical properties of austenitic stainless steels at cryogenic temperatures. *Tetsu to Hagane* **71**(14), 1647–1654, https://doi.org/10.2355/tetsutohagane1955.71.14_1647 (1985).
136. Mimino, T., Kinoshita, K., Shinoda, T. & Minegishi, I. The changes of structure and mechanical properties of 18-8 series stainless steels after prolonged aging. *Transactions of the Iron and Steel Institute of Japan* **9**(6), 472–482, https://doi.org/10.2355/isijinternational1966.9.472 (1969).
137. Zhong, Y. *et al*. Additive manufacturing of 316L stainless steel by electron beam melting for nuclear fusion applications. *Journal of Nuclear Materials* **486**, 234–245, https://doi.org/10.1016/j.jnucmat.2016.12.042 (2017).
138. Mirzababaei, S., Paul, B. K. & Pasebani, S. Microstructure-property relationship in binder jet produced and vacuum sintered 316L. *Additive Manufacturing* **53**, 102720, https://doi.org/10.1016/j.addma.2022.102720 (2022).
139. Mandiang, Y., Ciss, A., Sissoko, G. & Cizeron, G. Influence of thermal aging on microstructural evolution and mechanical properties in titanium modified type 316 stainless steel containing phosphorus. *Materials Science and Technology* **17**(3), 315–320, https://doi.org/10.1179/026708301773002527 (2001).
140. Bharasi, N. S. *et al*. Microstructure, corrosion, and mechanical properties characterization of AISI type 316L(N) stainless steel and modified 9Cr-1Mo steel after 40,000 h of dynamic sodium exposure at 525 °C. *Journal of Nuclear Materials* **516**, 84–99, https://doi.org/10.1016/j.jnucmat.2019.01.012 (2019).
141. Ambade, S. *et al*. Experimental investigation of microstructural, mechanical, and corrosion properties of 316L and 202 austenitic stainless steel joints using cold metal transfer welding. *Journal of Materials Research and Technology* **27**, 5881–5888, https://doi.org/10.1016/j.jmrt.2023.11.091 (2023).
142. Sireesha, M., Albert, S. K., Shankar, V. & Sundaresan, S. A comparative evaluation of welding consumables for dissimilar welds between 316LN austenitic stainless steel and Alloy 800. *Journal of Nuclear Materials* **279**(1), 65–76, https://doi.org/10.1016/S0022-3115(99)00275-5 (2000).
143. Goto, T., Naito, T. & Yamaoka, T. A study on NDE method of thermal aging of cast duplex stainless steels. *Nuclear Engineering and Design* **182**(2), 181–192, https://doi.org/10.1016/S0029-5493(97)00360-9 (1998).
144. Snyder, C. *et al*. Material characterization study of laser powder bed fusion type 316L stainless steel with process parameter modifications to promote isotropy. In N. Shamsaei, N. Hrabe & M. Seifi (Eds.), *Progress in Additive Manufacturing* 2021 (pp. 123–139). West Conshohocken, PA: ASTM International. https://doi.org/10.1520/STP1644202200024 (2022).
145. Li, H. L., Liu, D., Yan, Y. T., Guo, N. & Feng, J. C. Microstructural characteristics and mechanical properties of underwater wet flux-cored wire welded 316L stainless steel joints. *Journal of Materials Processing Technology* **238**, 423–430, https://doi.org/10.1016/j.jmatprotec.2016.08.001 (2016).

146. Tomar, B. & Shiva, S. Microstructural and mechanical properties examination of SS316L-Cu functionally graded material fabricated by wire arc additive manufacturing. *CIRP Journal of Manufacturing Science and Technology* **50**, 26–39, https://doi.org/10.1016/j.cirpj.2024.02.002 (2024).
147. Vora, J. *et al*. (Experimental investigations on mechanical properties of multi-layered structure fabricated by GMAW-based WAAM of SS316L. *Journal of Materials Research and Technology* **20**, 2748–2757, https://doi.org/10.1016/j.jmrt.2022.08.074 (2022).
148. Saucedo-Muñoz, M. L. *et al*. Effect of precipitation on cryogenic toughness in isothermally aged austenitic stainless steel. *Metallurgical Science and Heat Treatment* **58**(11–12), 707–711, https://doi.org/10.1007/s11041-017-0082-4 (2017).
149. Jansa, J. *et al*. Corrosion and material properties of 316L stainless steel produced by material extrusion technology. *Journal of Manufacturing Processes* **88**, 232–245, https://doi.org/10.1016/j.jmapro.2023.01.035 (2023).
150. Xia, X. *et al*. Correlation between microstructure evolution and mechanical properties of 50 mm 316L electron beam welds. *Fusion Engineering and Design* **147**, 111245, https://doi.org/10.1016/j.fusengdes.2019.111245 (2019).
151. Samuel, K. G., Sreenivasan, P. R., Ray, S. K. & Rodriguez, P. Evaluation of ageing-induced embrittlement in an austenitic stainless steel by instrumented impact testing. *Journal of Nuclear Materials* **150**(1), 78–84, https://doi.org/10.1016/0022-3115(87)90095-X (1987).
152. Kumar, S., Murugan, N. & Ramachandran, K. K. Effect of friction stir welding on mechanical and microstructural properties of AISI 316L stainless steel butt joints. *Welding in the World* **63**, 137–150, https://doi.org/10.1007/s40194-018-0621-7 (2019).
153. Amudarasan, N. V., Palanikumar, K. & Shanmugam, K. Mechanical properties of AISI 316L austenitic stainless steels welded by GTAW. *Advanced Materials Research*, **849**, 50–57, www.scientific.net/amr.849.50 (2013).
154. Saito, S. *et al*. Neutron irradiation effect on the mechanical properties of type 316L SS welded joints. *Journal of Nuclear Materials* **307–311**(Part 2), 1573–1577, https://doi.org/10.1016/S0022-3115(02)01021-8 (2002).
155. Que, Z., Chang, L., Saario, T. & Bojinov, M. Localised electrochemical processes on laser powder bed fused 316 stainless steel with various heat treatments in high-temperature water. *Additive Manufacturing* **60**(Part A), 103205, https://doi.org/10.1016/j.addma.2022.103205 (2022).
156. Bharasi, N. S., Pujar, M. G., Thyagarajan, K. & others Changes in microstructural and mechanical properties of AISI type 316LN stainless steel and modified 9Cr-1Mo steel on long-term exposure to flowing sodium in a bi-metallic sodium loop. *Metallurgical and Materials Transactions A* **46**, 6065–6080, https://doi.org/10.1007/s11661-015-3147-2 (2015).
157. Takahashi, H., Saito, K., Shoji, T., Date, K. & Suzuki, M. Reactor surveillance test and fracture mechanics evaluation of irradiation embrittlement in reactor pressure vessel steels. *Journal of Engineering Materials and Technology* **102**(4), 317–326, https://doi.org/10.1115/1.3224818 (1980).
158. Lou, X., Andresen, P. L. & Rebak, R. B. Oxide inclusions in laser additive manufactured stainless steel and their effects on impact toughness and stress corrosion cracking behavior. *Journal of Nuclear Materials* **499**, 182–190, https://doi.org/10.1016/j.jnucmat.2017.11.036 (2018).
159. Saravanan, P. *et al*. Mechanical properties and corrosion behaviour of developed high nitrogen high manganese stainless steels. *Materialwissenschaft und Werkstofftechnik* **54**(6), 615–624, https://doi.org/10.1002/mawe.202100178 (2023).
160. Schill, R.H., Forget, P. & Catherine, C.S. Correlation between Charpy-V and sub-size Charpy tests results for an un-irradiated low alloy RPV ferritic steel. https://www.gruppofrattura.it/ocs/index.php/esis/ECF13/paper/view/8423/4871 (2013).
161. Kolluri, M. *et al*. Mechanical properties and microstructure of long-term thermal aged WWER 440 RPV steel. *Journal of Nuclear Materials* **486**, 138–147, https://doi.org/10.1016/j.jnucmat.2017.01.007 (2017).
162. Kolluri, M. *et al*. Influence of Ni-Mn contents on the embrittlement of PWR RPV model steels irradiated to high fluences relevant for LTO beyond 60 years. *Journal of Nuclear Materials*, 553, 153036. https://doi.org/10.1016/j.jnucmat.2021. 153036 (2021).
163. Automeris. *WebPlotDigitizer*. https://apps.automeris.io/wpd4/ (2024).
164. Lee, I. *et al*. Dataset of Charpy V-notch impact test records of nuclear structural materials. (Version v1) [Data set]. *Materials Cloud Archive* **2025**, 30, https://doi.org/10.24435/materialscloud:p6-5y (2025).
165. Towers, O. L. Charpy V-Notch Tests: Influences of Striker Geometry and of Specimen Thickness. *Research Report* **219**/1983, The Welding Institute. (1983).
166. Zhang, W. Technical problem identification for the failures of the Liberty Ships. *Challenges* **7**(2), 20, https://doi.org/10.3390/challe7020020 (2016).
167. Bajramović, E., Islamović, F. Testing the impact energy and determination of the brittleness temperature of the welded joint of steel A516 Gr.70. *IOP Conference Series: Materials Science and Engineering* **1298**(1), https://doi.org/10.1088/1757-899X/1298/1/012003 (2023).


## Acknowledgements

This work was supported through the INL Laboratory Directed Research& Development (LDRD) Program under DOE Idaho Operations Office Contract DE-AC07-05ID14517 (project tracking number 24A1081-149). Accordingly, the publisher, by accepting the article for publication, acknowledges that the U.S. Government retains a nonexclusive, paid-up, irrevocable, worldwide license to publish or reproduce the published form of this manuscript or allow others to do so, for U.S. Government purposes.

## Author contributions

R.S., F.X. and J.M. developed the concept for the study. I.L. led the literature search and data extraction effort, and was supported by Y.T., F.X. and A.V. R.S. and J.R. analyzed the data and contributed to the data validation. I.L. and Y.K. performed data organization and cleaning to create the final dataset. I.L., Y.K., J.M., A.V. and F.X. drafted the first version of the manuscript. All authors reviewed the manuscript.

## Competing interests

The authors declare no competing interests.

## Additional information

**Correspondence** and requests for materials should be addressed to A.V. or R.S.